

Transient seepage model for saturated–unsaturated soil systems: a geotechnical engineering approach

L. LAM, D. G. FREDLUND, AND S. L. BARBOUR

Department of Civil Engineering, University of Saskatchewan, Saskatoon, Sask., Canada S7N 0W0

Received September 11, 1986

Accepted May 26, 1987

A two-dimensional finite element model is proposed to simulate transient seepage for complex groundwater flow systems. The complete soil system is treated as a continuum encompassing flow in both saturated and unsaturated zones. In the unsaturated zone, the air phase is assumed to be continuous and open to atmospheric pressure. The coefficient of permeability of the unsaturated soil is assumed to be a function of pore-water pressure.

The governing differential equation is derived within a framework familiar to geotechnical engineers. The stress state variables and the constitutive relationships for an unsaturated soil are used in the derivation. The finite element solution to the governing differential equation is based on the Galerkin weighted-residual method. The nonlinearity of the equation is solved by iterative procedures.

The finite element formulation is implemented into a computer model named TRASEE. The model can be applied to a wide variety of problems involving complex boundary conditions and geometries with arbitrary degrees of heterogeneity and anisotropy. Example problems are presented to demonstrate the capabilities of the model. The results indicate that the quantity of water flow in the unsaturated zone may be substantial, and that the phreatic line is not a flow line. It has been found that the traditional "saturated-only" flow-net technique can be approximated as a special case to the proposed saturated–unsaturated model.

Key words: unsaturated flow, finite element model, phreatic line, permeability function, transient seepage.

L'on propose un modèle à deux dimensions en éléments finis pour simuler l'infiltration transitoire pour des systèmes complexes d'écoulement d'eau souterraine. Le système sol complet est traité comme un milieu continu d'écoulement dans la zone tant saturée que non saturée. Dans la zone saturée, l'on suppose que la phase gazeuse est continue et ouverte à la pression atmosphérique. Le coefficient de perméabilité du sol non saturé est considéré comme étant une fonction de la pression interstitielle.

L'équation différentielle de base est familière aux ingénieurs géotechniciens. Les variables de l'état de contrainte et les équations de comportement pour un sol non saturé sont utilisées dans la dérivation. La solution par éléments finis de l'équation différentielle de base est fondée sur la méthode Galerkin de résidu pondéré. La non-linéarité de l'équation est résolue par des procédés itératifs.

La formulation des éléments finis est exécutée dans un modèle d'ordinateur nommé TRASEE. Le modèle peut être appliqué à une grande variété de problèmes impliquant des conditions aux limites complexes et des géométries avec des degrés arbitraires d'hétérogénéité et d'anisotropie. Des problèmes sont présentés en exemples pour démontrer le potentiel de ce modèle. Les résultats indiquent que la quantité d'écoulement d'eau dans la zone non saturée peut être substantielle, et que la ligne phréatique n'est pas une ligne d'écoulement. Il a été démontré que la technique du réseau d'écoulement saturé traditionnel peut être considéré approximativement comme un cas spécial du modèle proposé saturé – non saturé.

Mots clés : écoulement non saturé, modèle en éléments finis, ligne phréatique, fonction de perméabilité, infiltration transitoire.

[Traduit par la revue]

Can. Geotech. J. 24, 565–580 (1987)

Introduction

In geotechnical engineering, seepage analysis may be of interest with respect to slope stability analysis, groundwater contamination control, and the design of hydraulic structures. Since Casagrande's (1937) classic paper "Seepage through dams," seepage problems in geotechnical engineering have been generally solved by sketching flow nets. This method is based on the assumption that water flows only in the saturated zone. This method of solution is practical for simple steady state problems where the boundary of the flow region is clearly defined and the soil conditions are not too complex. However, many seepage problems of practical interest are complex, and a flow-net solution is not feasible.

With the development of high-speed digital computers, numerical methods are increasingly used in solving seepage problems. Some of the first attempts at modelling seepage using the finite element method also considered water flow only in the saturated zone. An example is the finite element flow model proposed by Taylor and Brown (1967). In this

"saturated-only" approach, the phreatic line was assumed to be the upper boundary of the flow region for unconfined flow problems. In order to obtain the location of the phreatic line, a trial and error procedure is used to search for a surface that has both zero water pressure along it and zero flow across it. For each trial, the location of the phreatic line is readjusted, and a new mesh is constructed. This method is tedious, and it is also based on the erroneous assumption that the phreatic line is the uppermost flow boundary.

A saturated–unsaturated model would appear to be superior to the saturated-only model. By considering water flow in both the saturated and unsaturated zones, the actual ground surface (rather than the phreatic line) can be used as the uppermost boundary. The phreatic line is obtained by joining points of zero water pressure in the flow region. The finite difference model proposed by Freeze (1971a) is an example of a saturated–unsaturated flow model. This model allows the calculation of flow and hydraulic heads in the unsaturated zone. It also allows the modelling of situations with a surface

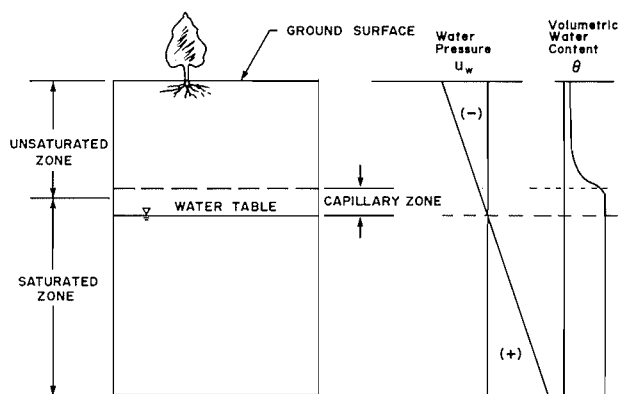


FIG. 1. A saturated-unsaturated soil profile under hydrostatic conditions.

flux. As well, there is no need to adjust the mesh during the solution of the problem.

Much of the research concerning unsaturated flow has been undertaken by soil scientists. Geotechnical engineers have often accepted formulations from researchers with diverse backgrounds without evaluating the assumptions and objectives of their formulation. This paper presents the development of a transient finite element seepage model using an approach consistent with that used by geotechnical engineers. The concepts pertinent to the understanding of unsaturated flow are reviewed. The general governing differential equation for transient seepage is derived and the finite element solution to the equation is presented.

Review of unsaturated flow concepts

Unsaturated flow is an example of multiphase flow through a porous media. Two phases, air and water, coexist in the pore channels. Two partial differential equations are required to rigorously describe the flow of air and water in unsaturated soil. Problems of this kind are referred to as two-phase flow problems (Fredlund 1981). However, for most seepage problems encountered in geotechnical engineering, only flow in the water phase of the unsaturated zone is of practical interest. This "single-phase" flow approach is used in this paper. The fundamental assumption is that the air phase is continuous and the pore-air pressure is equal to atmospheric pressure. This is generally the case when the degree of saturation is less than approximately 85%. In the case where the degree of saturation is larger than 85%, the air phase is occluded. However, the occluded air pressure will still be essentially atmospheric and will not introduce significant error into the "single-phase" flow approach. Freeze and Cherry (1979) stated that "the single-phase approach to unsaturated flow leads to techniques of analysis that are accurate enough for almost all practical purposes."

Soils are porous materials, with water being free to flow through the interconnected pores between the solid particles. Regardless of the degree of saturation of the soil, water flows under the influence of a hydraulic gradient. The driving gradient can be identified by Bernoulli's theorem. Since seepage velocities in soils are normally small, the velocity head can be neglected, and the driving force is the sum of pore-water pressure head and elevation head:

$$[1] \quad h = \frac{u_w}{\rho_w g} + z$$

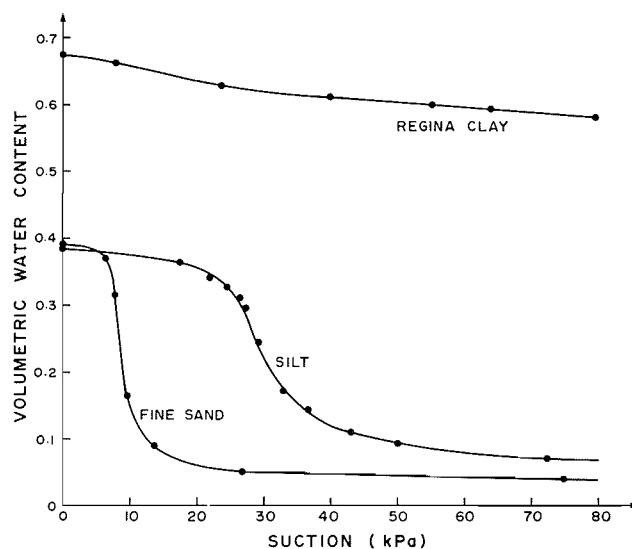


FIG. 2. Moisture retention curve for fine sand, silt, and Regina clay.

where h = total head, u_w = pore-water pressure, z = elevation head above an arbitrary datum, ρ_w = density of water, and g = acceleration due to gravity.

The flow of water through a soil mass can be described using Darcy's law:

$$[2] \quad q = ki$$

where q = discharge per unit area, i = potential gradient, and k = coefficient of permeability (or hydraulic conductivity). Darcy's law, which was originally derived for saturated soil, can equally be applied to the flow of water through an unsaturated soil (Richards 1931; Childs and Collis-George 1950). The only difference is that for flow through an unsaturated soil, the coefficient of permeability is no longer a constant but is a function of the matric suction of the soil.

Figure 1 illustrates the pore-water pressure and moisture distribution within a soil profile under hydrostatic conditions. The water table (i.e., phreatic line) is an imaginary surface where the pore-water pressure is zero. Water may flow up and down across the water table if there is a hydraulic gradient between the saturated and unsaturated zones. Below the water table, the pore-water pressure is positive and increases linearly with depth. Above the water table, the pore-water pressure is negative and decreases with height. The amount of water retained in the unsaturated zone of a particular soil is a function of matric suction ($u_a - u_w$) of the soil (Fredlund and Morgenstern 1977). Since the pore-air pressure is atmospheric, the matric suction is also equal to the absolute value of the negative pore-water pressure.

Figure 2 shows the laboratory retention curve for fine sand, silt, and Regina clay obtained by Ho (1979). These retention curves were obtained using Tempe pressure cells. The operating principles and the testing procedures can be found in the "Operating instructions for Tempe pressure cell" by Soil Moisture Equipment Corporation, Santa Barbara, California. In order to consider flow in both the saturated and unsaturated zones of a flow regime, the permeability of the soil at all points in both the saturated and unsaturated zones must be known. The saturated coefficient of permeability can be obtained using standard laboratory and field procedures. However, the direct measurement of the unsaturated permeability is often expen-

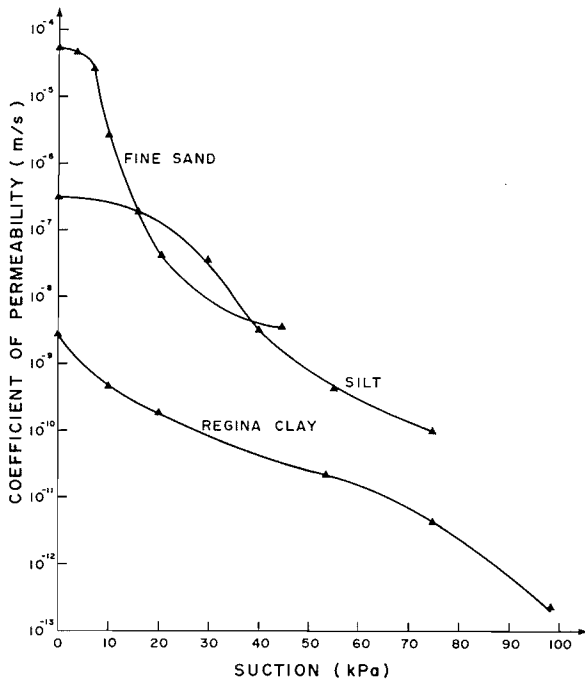


FIG. 3. Unsaturated permeability function of fine sand, silt, and Regina clay.

sive and difficult to conduct. Considerable research has been done on evaluating the unsaturated permeability of a soil based upon its soil moisture retention curve, which is relatively simple to obtain (Childs and Collis-George 1950; Marshall 1958; Green and Corey 1971; Elzeftawy and Cartwright 1981). It has been concluded that this method generally gives reliable predictions of experimentally measured permeability values.

The moisture retention curve of a soil is of primary importance in understanding the transient flow of water in the unsaturated zone. The slope of the curve represents the storage characteristics of the soil (i.e., the m_2^w value in [9]). The slope indicates the amount of water taken on or released by the soil as a result of a change in the pore-water pressure. The moisture retention curve of a soil also provides a quantitative means of calculating the permeability function of the soil using procedures developed by Green and Corey (1971) and other researchers.

The retention curves and the calculated permeability functions as presented in Figs. 2 and 3 are typical for materials of different grain sizes. A coarser material (e.g., sand) will desaturate faster than a finer material (e.g., clay). Consequently, as anticipated, a sandy material will have a steeper permeability function than a clayey material.

General governing equation

Terzaghi's (1943) one-dimensional consolidation theory for saturated soils introduced an approach to seepage problems that was particularly suitable to geotechnical engineering. The governing partial differential equation was derived by equating the net flow quantity from a soil element to the time derivative of the constitutive equation for the soil.

Fredlund and Morgenstern (1977) proposed the use of two independent stress state variables, $(\sigma - u_a)$ and $(u_a - u_w)$, to describe the state of stress for an unsaturated soil. Constitutive equations relating the volume change in the soil structure and

fluid phases to stress state variable changes were also proposed (Fredlund and Morgenstern 1976).

The net flow through a two-dimensional element of unsaturated soil can be expressed as

$$[3] \quad \Delta q = \frac{\partial \theta_w}{\partial t} = - \frac{\partial}{\partial x} \left(k_x \frac{\partial h}{\partial x} \right) - \frac{\partial}{\partial y} \left(k_y \frac{\partial h}{\partial y} \right)$$

The constitutive equation for the water phase of an isotropic unsaturated soil is

$$[4] \quad d\theta_w = m_1^w d(\sigma - u_a) + m_2^w d(u_a - u_w)$$

where m_1^w = slope of the $(\sigma - u_a)$ versus θ_w plot when $d(u_a - u_w)$ is zero, m_2^w = slope of the $(u_a - u_w)$ versus θ_w plot when $d(\sigma - u_a)$ is zero, σ = total stress in the x - and (or) y -direction, u_a = pore-air pressure, and u_w = pore-water pressure.

Since m_1^w and m_2^w can be assumed to be constant for a particular time step during the transient process, the time derivative of the constitutive equation can be expressed as

$$[5] \quad \frac{\partial \theta_w}{\partial t} = m_1^w \frac{\partial(\sigma - u_a)}{\partial t} + m_2^w \frac{\partial(u_a - u_w)}{\partial t}$$

Combining [3] and [5] gives

$$[6] \quad - \frac{\partial}{\partial x} \left(k_x \frac{\partial h}{\partial x} \right) - \frac{\partial}{\partial y} \left(k_y \frac{\partial h}{\partial y} \right) = m_1^w \frac{\partial(\sigma - u_a)}{\partial t} + m_2^w \frac{\partial(u_a - u_w)}{\partial t}$$

If it is assumed that no external loads are added to the soil mass during the transient process, and that the air phase is continuous in the unsaturated zone (i.e., $\partial\sigma/\partial t = 0$ and $\partial u_a/\partial t = 0$), [6] can be simplified as follows:

$$[7] \quad \frac{\partial}{\partial x} \left(k_x \frac{\partial h}{\partial x} \right) + \frac{\partial}{\partial y} \left(k_y \frac{\partial h}{\partial y} \right) = m_2^w \frac{\partial u_w}{\partial t}$$

Expressing the pore-water pressure term in [7] in terms of total head, the governing differential equation for transient seepage can therefore be written as follows:

$$[8] \quad \frac{\partial}{\partial x} \left(k_x \frac{\partial h}{\partial x} \right) + \frac{\partial}{\partial y} \left(k_y \frac{\partial h}{\partial y} \right) = \rho_w g m_2^w \frac{\partial h}{\partial t}$$

After incorporating anisotropic soil conditions where the direction of the major coefficient of permeability is inclined at an arbitrary angle to the x -axis, [8] becomes

$$[9] \quad \frac{\partial}{\partial x} \left(k_{xx} \frac{\partial h}{\partial x} + k_{xy} \frac{\partial h}{\partial y} \right) + \frac{\partial}{\partial y} \left(k_{yx} \frac{\partial h}{\partial x} + k_{yy} \frac{\partial h}{\partial y} \right) = \rho_w g m_2^w \frac{\partial h}{\partial t}$$

where $k_{xx} = k_1 \cos^2 \alpha + k_2 \sin^2 \alpha$, $k_{yy} = k_1 \sin^2 \alpha + k_2 \cos^2 \alpha$, $k_{xy} = k_{yx} = (k_1 - k_2) \sin \alpha \cos \alpha$, k_1 = major coefficient of permeability, k_2 = minor coefficient of permeability, and α = inclined angle between k_1 and the x -axis.

The above governing partial differential flow equation (i.e., [9]) has been developed in a manner most familiar to geotechnical engineers. The equation has been derived on the basis of unsaturated flow theory (Fredlund 1981) and can be used to describe continuous flow in saturated-unsaturated soil systems. The term m_2^w represents the rate at which a soil will absorb or release water when there is a change in matric suc-

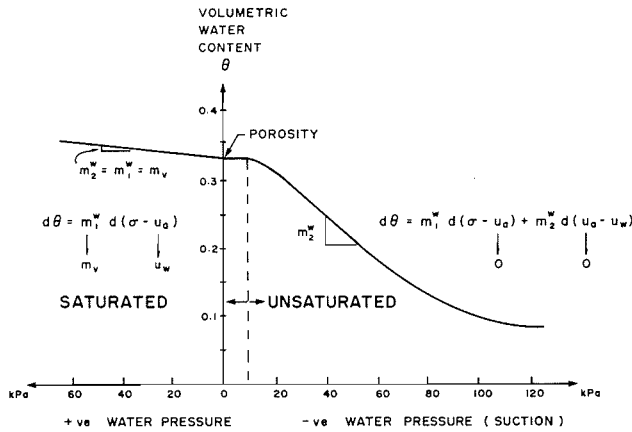


FIG. 4. Moisture retention curve and m_2^w for saturated-unsaturated soil.

tion. Figure 4 illustrates the variation in the value of the term m_2^w as the soil changes from saturated to unsaturated conditions. The value of m_2^w is equal to the slope of the water retention curve. Under the assumptions of a constant total stress and a pore-air pressure equal to the pore-water pressure, m_2^w becomes equal to m_1^w in the saturated zone. The m_1^w value is equivalent to the coefficient of volume change, m_v , common to saturated soil mechanics.

Finite element formulation

With the advance of high-speed digital computers, numerical methods provide practical solutions to complex seepage problems. The finite element method is the most powerful and widely used numerical method for two-dimensional problems. The following section presents the finite element formulation for the governing equation.

The Galerkin solution to [9] is given by the following integrals over the area and boundary surface of a triangular element (Lam 1983):

$$[10] \int_A [B]^T [K] [B] dA [h^n] + \int_A [L]^T \lambda [L] dA \frac{\partial [h^n]}{\partial t} - \int_s [L]^T q ds = 0$$

where

$$[B] = \frac{1}{2A} \begin{bmatrix} y_2 - y_3 & y_3 - y_1 & y_1 - y_2 \\ x_3 - x_2 & x_1 - x_3 & x_2 - x_1 \end{bmatrix}$$

with x_1, y_1 equal to the Cartesian coordinates of the nodes of the element;

$$[K] = \begin{bmatrix} k_{xx} & k_{xy} \\ k_{yx} & k_{yy} \end{bmatrix}$$

with $k_{xx}, k_{xy}, k_{yx}, k_{yy}$ equal to the components of the permeability tensor for the element;

$$[h^n] = \begin{bmatrix} h_1 \\ h_2 \\ h_3 \end{bmatrix}$$

with h_i equal to the total head at the element nodes;

$$[L]^T = [L_1, L_2, L_3]$$

with L_i equal to the area coordinates of the element;

- $\lambda = \rho_w g m_2^w$
- $q =$ flow across the perimeter of the element
- $A =$ area of the element
- $S =$ perimeter of the element
- $t =$ time

After numerical integration, [10] can be simplified as follows:

$$[11] [D][h^n] + [E][\dot{h}^n] = [F]$$

where

$$[D] = [B]^T [K] [B] A$$

is the stiffness matrix;

$$[E] = \frac{\lambda A}{12} \begin{bmatrix} 2 & 1 & 1 \\ 1 & 2 & 1 \\ 1 & 1 & 2 \end{bmatrix}$$

is the capacitance matrix;

$$[F] = \frac{ql}{2} \begin{bmatrix} 1 \\ 1 \\ 0 \end{bmatrix} \text{ or } \frac{ql}{2} \begin{bmatrix} 1 \\ 0 \\ 1 \end{bmatrix} \text{ or } \frac{ql}{2} \begin{bmatrix} 0 \\ 1 \\ 1 \end{bmatrix}$$

is the flux vector reflecting the boundary conditions;

$$[\dot{h}^n]$$

is the time derivative of nodal total head.

For transient seepage, the time derivative of [11] can be approximated by a finite difference procedure. Consequently, the relationship between the nodal heads of an element in two successive time steps can be expressed by the following equations:

$$[12] \left([D] + \frac{2[E]}{\Delta t} \right) [h^n]_{t+\Delta t} = \left(\frac{2[E]}{\Delta t} - [D] \right) [h^n]_t - 2[F]$$

$$[13] \left([D] + \frac{[E]}{\Delta t} \right) [h^n]_{t+\Delta t} = \frac{[E]}{\Delta t} [h^n]_t - [F]$$

Equation [12] is derived using the central difference approximation, and [13] is derived using the backward difference approximation. Both of the above time approximations are considered to be unconditionally stable. Generally, solutions based on the central difference approximation are found to be more accurate than those of the backward difference approximation. However, the backward difference approximation is found to be more effective in dampening the numerical oscillations frequently encountered in highly nonlinear flow systems (Neuman and Witherspoon 1971; Neuman 1973).

After the matrices for each element are formed, the algebraic equations for the whole system can be constructed and solved for nodal total head. However, due to the nonlinearity of the general seepage equation, an iterative procedure is required to obtain the correct nodal total heads. The iterative procedure involves a series of successive approximations. An initial estimate of the coefficient of permeability of an element is required in order to calculate a first approximation of the nodal total head. The computed nodal total head allows the calculation of the average pressure head of an element. Using the calculated average pressure heads and the input permeability function, an improved permeability value can be obtained for the element. The improved permeability value is used to com-

TABLE 1. Some transient seepage example problems modelled by TRASEE

Problem	Remark [†]
Earth dam	With a horizontal drain With an impervious lower boundary* With a center core of lower permeability With anisotropic soil conditions With infiltration at dam surface Reservoir level increased at a constant rate Instantaneous reservoir drawdown
Lagoon	No anisotropy in the soil With anisotropy, $\alpha = -30^\circ$ *
Hill slope	Homogeneous, infiltration and evapotranspiration Heterogeneous, infiltration and evapotranspiration
Sandbox model, Rulon and Freeze (1985)	With a horizontal layer of lower permeability, transient seepage with infiltration*

*Example problem presented in this paper.

[†]Reference: Lam (1983).

pute a new set of nodal total heads. The procedure is repeated until both the total head and permeability differences for each element for two successive iterations are smaller than specified tolerances.

The convergence rate is highly dependent on the degree of nonlinearity of the permeability function and the spatial discretization of the problem. A steep permeability function requires more iterations and a larger convergence tolerance. A finer discretization in both element size and time step will assist in obtaining convergence faster with a smaller tolerance. Generally, the solution will converge to a tolerance of less than 1% in 10 iterations.

The seepage equation is considered solved for one time step once the converged nodal total heads of the system are obtained. Secondary quantities at a particular time step, such as pore-water pressure, gradients, velocities, and flux quantities, can then be calculated based on the nodal total heads. The following equations apply:

The equation for nodal pore-water pressure,

$$[14] \quad [u_w]_t = ([h^n]_t - [z^n])\rho_w g$$

where $[z^n]$ = elevation at the nodes of the elements.

The equation for element gradient,

$$[15] \quad \begin{bmatrix} i_x \\ i_y \end{bmatrix}_t = [B][h^n]_t$$

The equation for element velocity,

$$[16] \quad \begin{bmatrix} v_x \\ v_y \end{bmatrix}_t = [K]_t [B][h^n]_t$$

The equation for flux,

$$[17] \quad [q_{ij}]_t = [D]_t (h_j^n - h_i^n)$$

where $[q_{ij}]_t$ = flux quantity to node i contributed from node j .

Implemented model, TRASEE

The finite element solution has been implemented into a computer program called TRASEE (Lam 1984). The computer facility used is a DIGITAL VAX 11/780 system in the College of Engineering, University of Saskatchewan, Saskatoon.

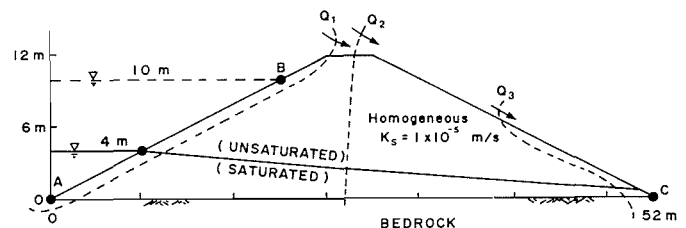


FIG. 5. Geometry and boundary conditions of example 1, seepage through earth dam.

The implemented two-dimensional program can model both transient and steady state seepage through saturated-unsaturated soil systems. It can accommodate complex geometries with arbitrary degrees of heterogeneity and anisotropy for 20 different soils. A discretized soil system of up to 1500 elements and 1000 nodes can be modelled. Three iterative techniques, including the Secant method, have also been incorporated to ensure convergence for highly nonlinear flow systems. Changing boundary conditions during a transient process can be accommodated by a prescribed step function. Special procedures are also included to automatically revise the boundary conditions along seepage faces and ponding surfaces. Flux quantities through any specified section of the flow system can be calculated. Furthermore, an auxiliary plotting and contouring program has also been developed for the presentation of computed results.

Example problems

The developed program has been used to solve a wide variety of transient seepage problems (Table 1). In this paper, results of three example problems are presented.

The basic information required for a finite element seepage analysis are the definition of the flow regime, which includes the spatial dimensions of the material boundaries, the definition of the boundary conditions, and the definition of material parameters. Subsurface investigation will be required to delineate the different material strata and the lowest boundary of the flow regime. Piezometric records and hydrological data are used to define the boundary conditions. In most cases, *in situ* or laboratory permeability tests, laboratory evaluation

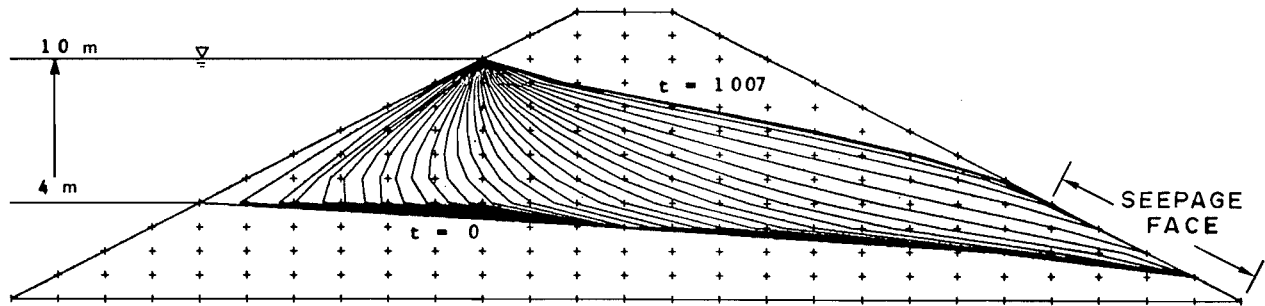


FIG. 6. Transient position of phreatic line from $t = 0$ to $t = 1007$ min.

of the moisture retention curves of the unsaturated materials, and the calculations of unsaturated permeability functions are required. In some cases, a knowledge of the soil types, typical moisture retention curves, and permeability functions can be used.

The first example illustrates transient seepage through a homogeneous earth dam with an impervious lower boundary. An analytical solution to this problem has been attempted by Brahma and Harr (1962). Their solution was based on the assumption that the free surface is the uppermost flow line. Later studies (Freeze 1971b; Papagianakis and Fredlund 1984) have shown that the free surface is a specific isobar in the pressure head field, which is a component of the hydraulic head field that controls the flow of water in both the saturated and unsaturated zones. When solving this problem using the developed saturated-unsaturated model, no assumption is required regarding the free surface. Therefore, the actual external soil boundaries can be used in the analysis.

Figure 5 shows the geometry and boundary conditions for the problem. The material is assumed to be sandy soil with a saturated coefficient of permeability of 1×10^{-5} m/s, and a m_2^w value of 0.0001 m²/kN. To better illustrate the flow in the unsaturated zone, a moderately steep permeability function (i.e., a decrease of 1 order of magnitude in permeability for every 5 m of negative pressure head) was assumed. Initially, the dam is at steady state conditions with the reservoir water level 4 m above datum. At time equal to zero, the water level is instantaneously raised to a level of 10 m. The water level remains constant at 10 m during the transient process.

Figure 6 illustrates the transient positions of the phreatic line as it advances from its initial steady state condition to a final steady state condition. Figures 7 and 8 present the computed results at times equal to 14, 107, 330, and 1007 min. Both the nodal total head plot and seepage velocity vector plot are presented for each time step.

The increase in reservoir level on the upstream face of the earth dam causes an increase in pore-water pressure with time. The change in pore-water pressure can be visualized by the changing position of the phreatic line and the equipotential lines at different times. The equipotential lines extend through the unsaturated zone as shown in Figs. 7 and 8, illustrating the presence of a hydraulic gradient and consequently water flow in the unsaturated zone. The fact that the phreatic line is not a flow line is confirmed by the seepage velocity vector plots. Figures 7 and 8 indicate that there is considerable flow across the phreatic line. These phenomena agree with the solution by Freeze (1971b).

Figure 9 shows the computed flux quantities Q_1 , Q_2 , and Q_3 through three sections (Fig. 6) of the earth dam during the transient process. Initially, the steady state flow quantity was equal

to 3×10^{-6} (m³·s⁻¹)/m as shown by Q_1 , Q_2 , and Q_3 . At times greater than zero, Q_1 increased rapidly to 3.5×10^{-4} (m³·s⁻¹)/m due to the instantaneous increase in the reservoir level. The quantity Q_1 then decreased gradually with time to a final steady state flux; Q_2 increased gradually to 3×10^{-5} (m³·s⁻¹)/m after 16 time steps and then decreased to a final steady state flux; Q_3 had no increase in flux during the early stages of the transient process, but after 10 time steps, began to increase gradually to the final steady state flux quantity.

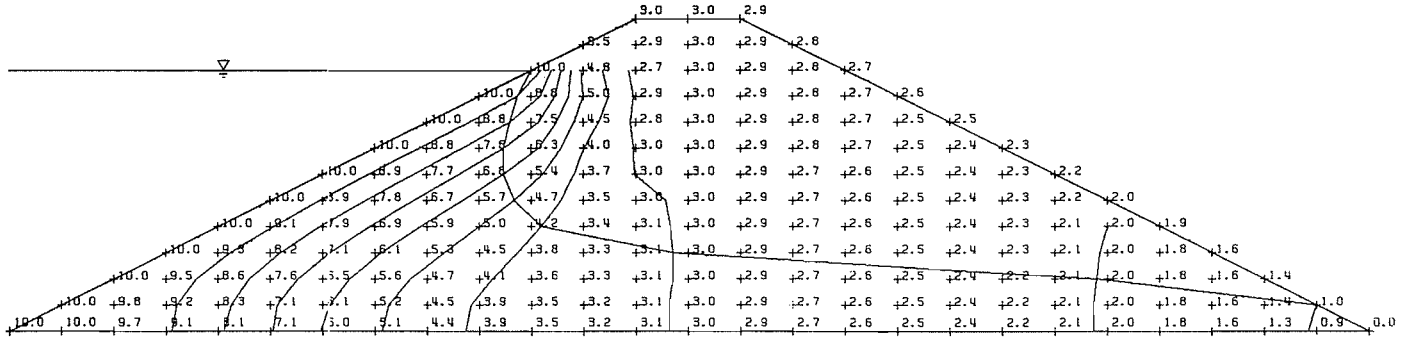
In this example, final steady state conditions were achieved after 32 time steps or an elapsed time of 1007 min. The computed flux quantity at final steady state conditions was 1.7×10^{-5} (m³·s⁻¹)/m. Using the flow-net technique, a flux of approximately 1.3×10^{-5} (m³·s⁻¹)/m was obtained. The difference in the two quantities is primarily due to the water flow through the unsaturated zone as computed by TRASEE. Unsaturated flow is not considered when using the flow-net technique. The use of a steeper permeability function will allow less water flow in the unsaturated zone, and the computed result will be closer to the flow-net solution (Lam 1983). The computed length of the seepage face above the downstream toe was 8.9 m. The flow-net solution gave a length of 6.5 m. When a steep permeability function is used, the computed length of the seepage face is reduced to 6.7 m. Consequently, the flow-net solution or the saturated-only model can be approximated as a special case of the saturated-unsaturated flow model.

The final steady state seepage condition achieved after 1007 min was also compared with the solution obtained from the steady state model called SEEP (Papagianakis and Fredlund 1984). The two models give almost identical solutions.

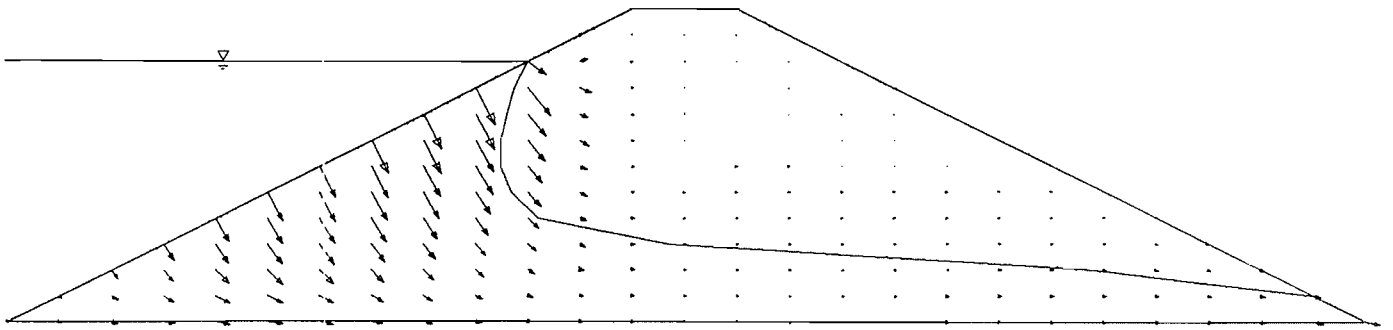
The second example, 2, illustrates transient groundwater seepage beneath a lagoon. Figure 10 illustrates the geometry and the boundary conditions of the problem. The material is assumed to be anisotropic with the major coefficient of permeability 10 times larger than the minor coefficient of permeability. The direction of the major coefficient of permeability is at an angle of -30° with the horizontal. The major coefficient of permeability of the soil at saturation was assumed to be 1×10^{-5} m/s. A 1 m thick liner was constructed on the bottom of the pond. The liner is assumed to be isotropic with a saturated coefficient of permeability equal to 1×10^{-6} m/s. The permeability function and m_2^w value used in example 1 are also used in this example.

An initial steady state condition with a water table located at 6.0 m below the ground surface was assumed. No flow conditions are assumed at the ground surface and the bottom boundary of the section. Furthermore, a hydrostatic condition was assumed to exist at both the left and right boundaries. At time equal to zero, the lagoon was filled with water. This pro-

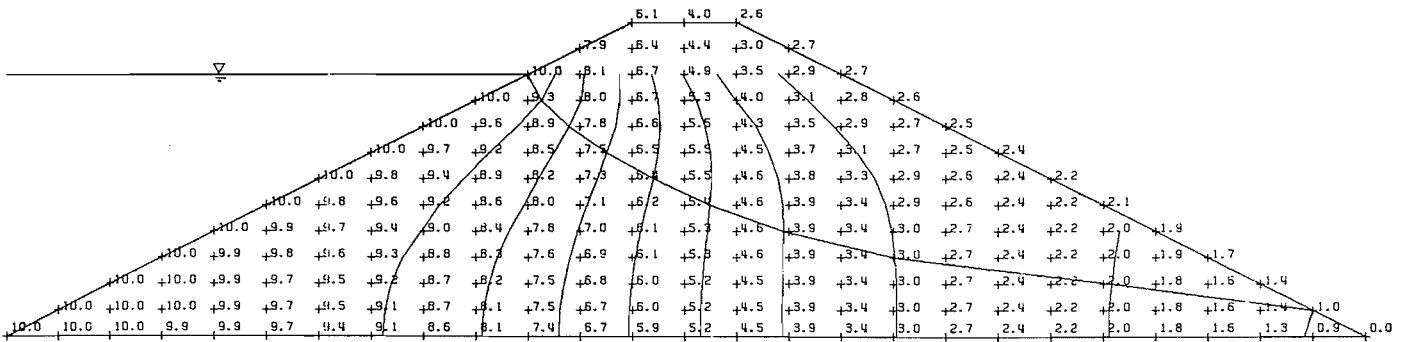
(a) NODAL TOTAL HEAD
t = 14 min



(b) SEEPAGE VELOCITY VECTOR
t = 14 min



(c) NODAL TOTAL HEAD
t = 107 min



(d) SEEPAGE VELOCITY VECTOR
t = 107 min

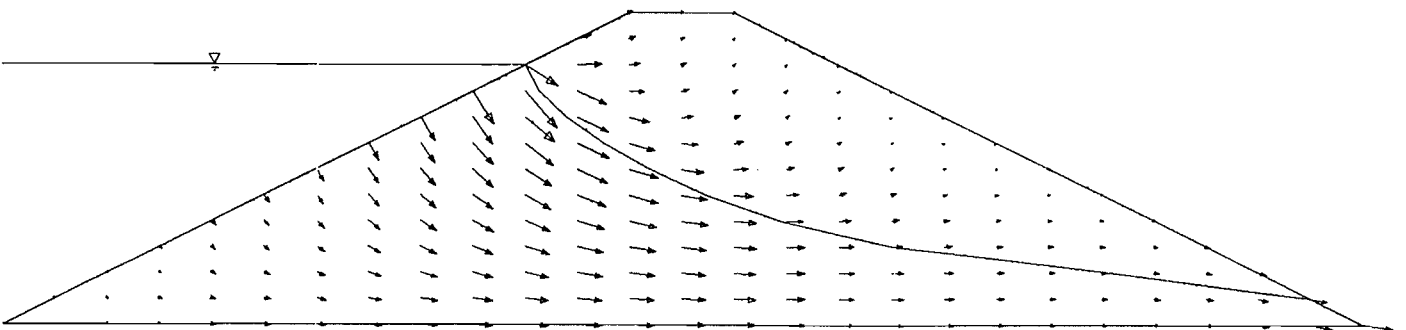
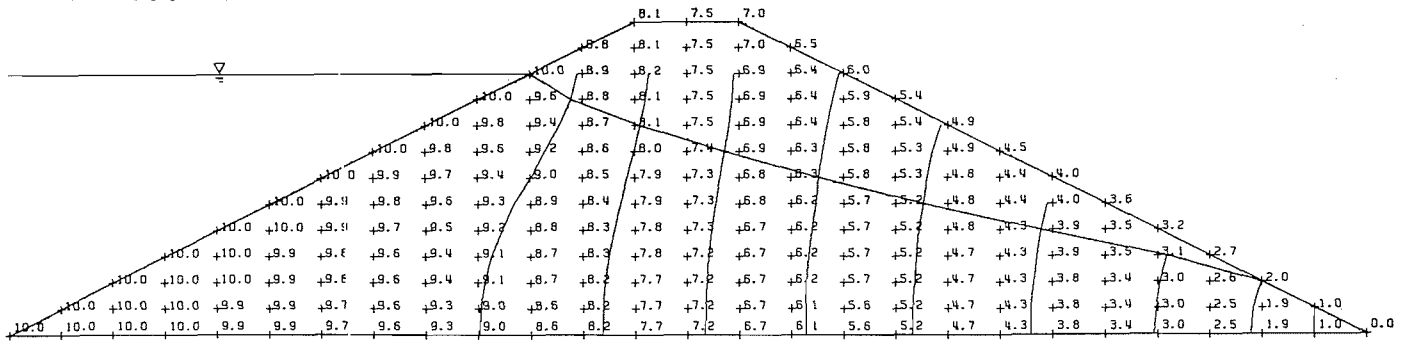
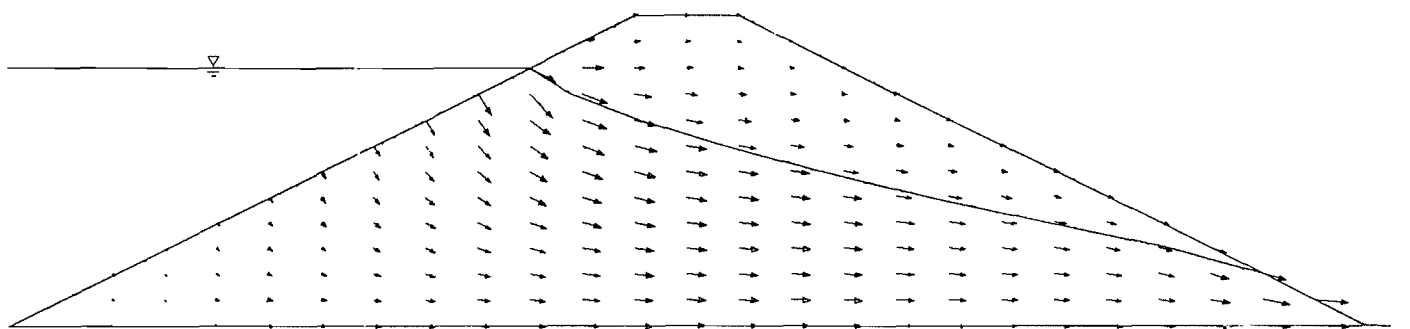


FIG. 7. Nodal total head and velocity vector plots at $t = 14$ and 107 min.

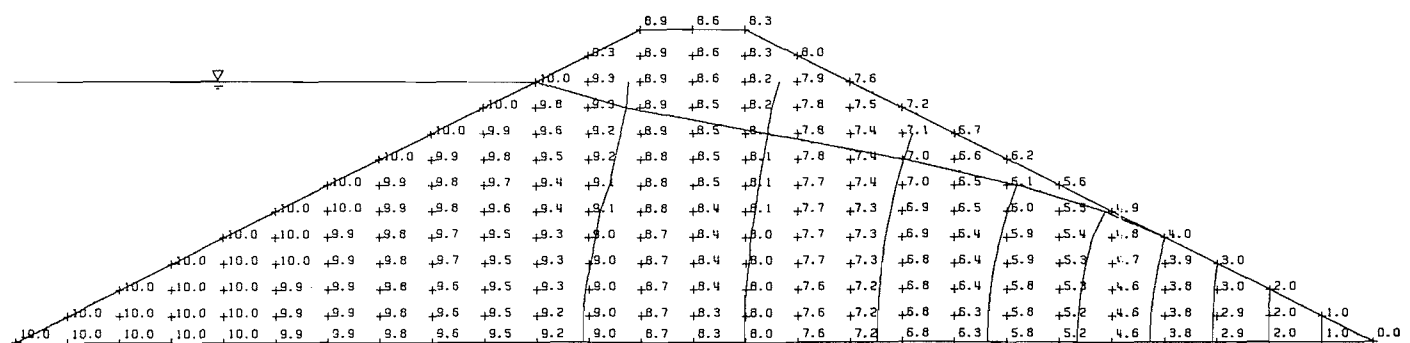
(a) NODAL TOTAL HEAD
t = 330 min



(b) SEEPAGE VELOCITY VECTOR
t = 330 min



(c) NODAL TOTAL HEAD
t = 1007 min



(d) SEEPAGE VELOCITY VECTOR
t = 1007 min

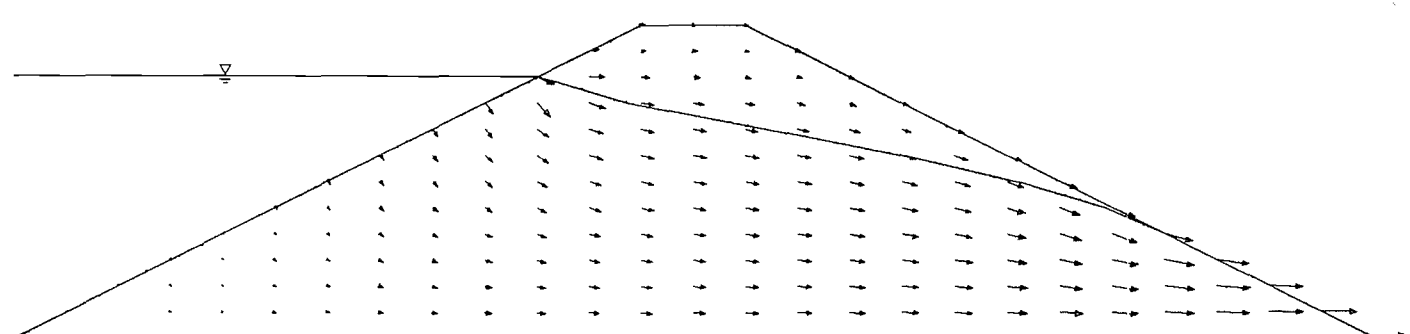


FIG. 8. Nodal total head and velocity vector plots at t = 330 and 1007 min.

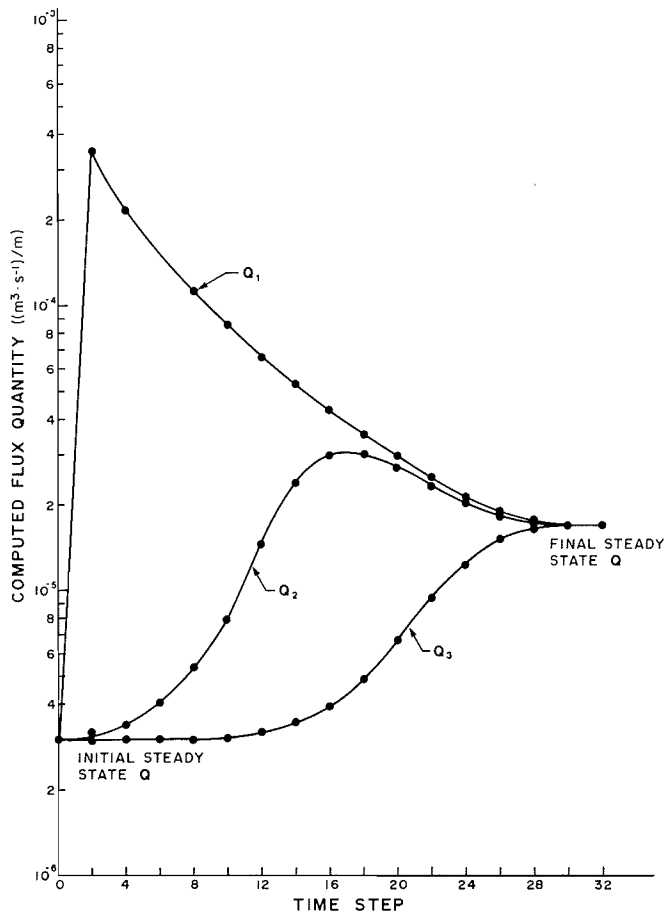


FIG. 9. Computed flux quantity at different time steps.

vided a water head of 1.0 m.

Figure 11 illustrates the transient position of the water table as seepage occurs from the lagoon. Figures 12 and 13 present solutions at different times. Both the pore-water pressure head and seepage velocity vector plots are presented. The contours show various pore-water pressure isobars.

It is difficult to visualize example 2 as a conventional saturated-only analysis. In the early stages of the transient process (Fig. 12a), water flows in the unsaturated zone only and the water table is unaffected. After 66.5 min, water from the lagoon reaches the water table, which begins to mound towards the lagoon (Figs. 12b and 13a). The groundwater mound builds up to the point where the seepage from the lagoon is balanced by the seepage leaving the left and right boundaries. In this example, the new steady state condition was achieved after 1316 min (Fig. 13b). If more water were to enter the flow system from the lagoon, the groundwater mound may build up higher and eventually come in contact with the lagoon (Lam 1983). The transient solution of example 2 compares satisfactorily with the transient processes described by McWhorter and Nelson (1979).

The effect of material anisotropy can be visualized from the seepage velocity vectors (Figs. 12 and 13). Under isotropic soil conditions, the flow system is symmetric with respect to the center line of the section. However, when the soil conditions are anisotropic, water flows along the axis of the major coefficient of permeability, causing an unsymmetric groundwater mound. Although the same boundary conditions are specified in both the left and right boundaries, water discharg-

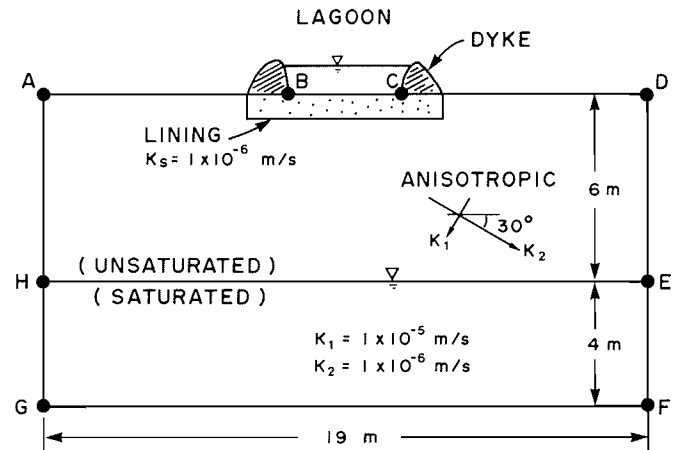


FIG. 10. Geometry and boundary conditions of example 2, seepage under lagoon.

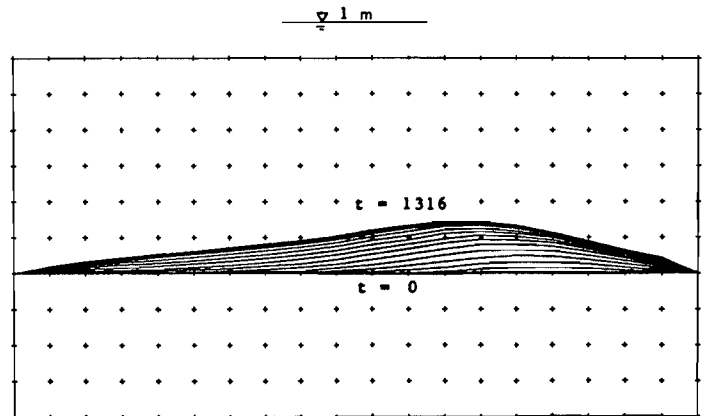
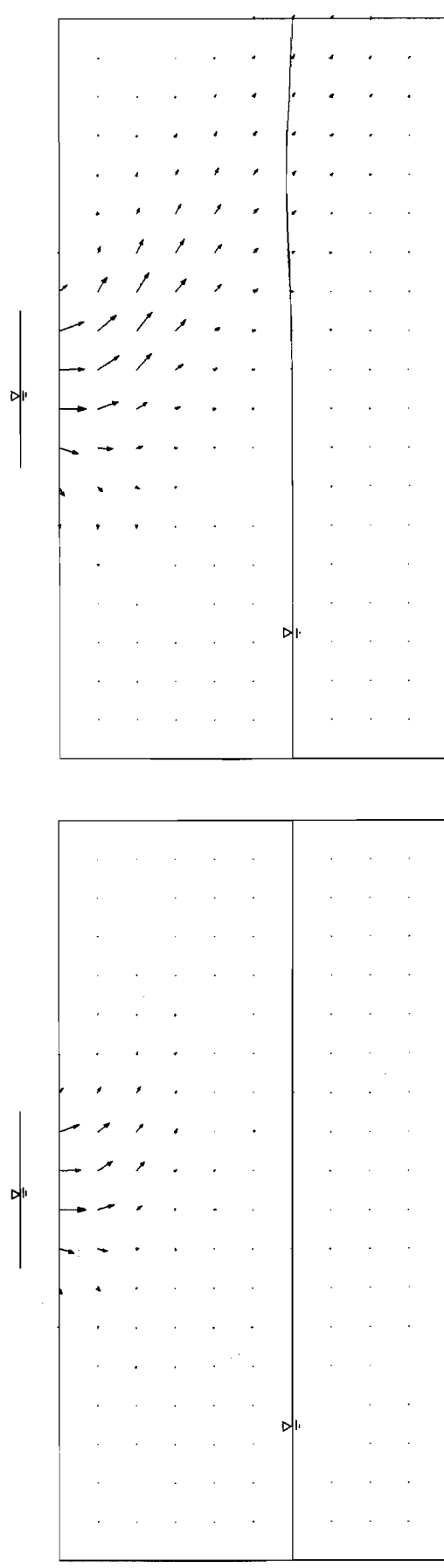
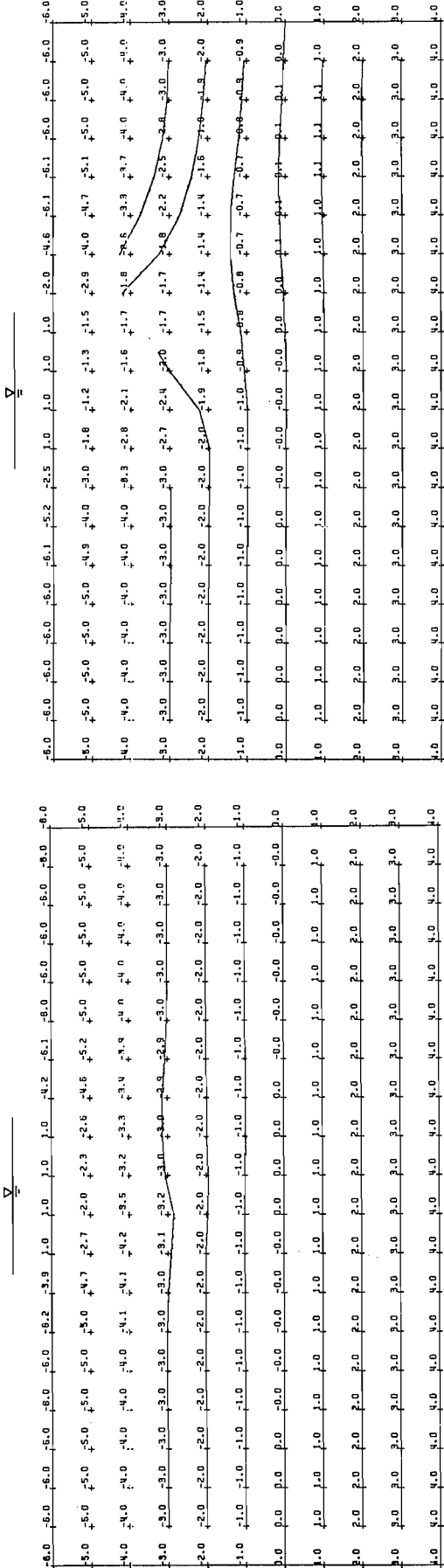


FIG. 11. Transient position of water table from $t = 0$ to $t = 1316$ min.

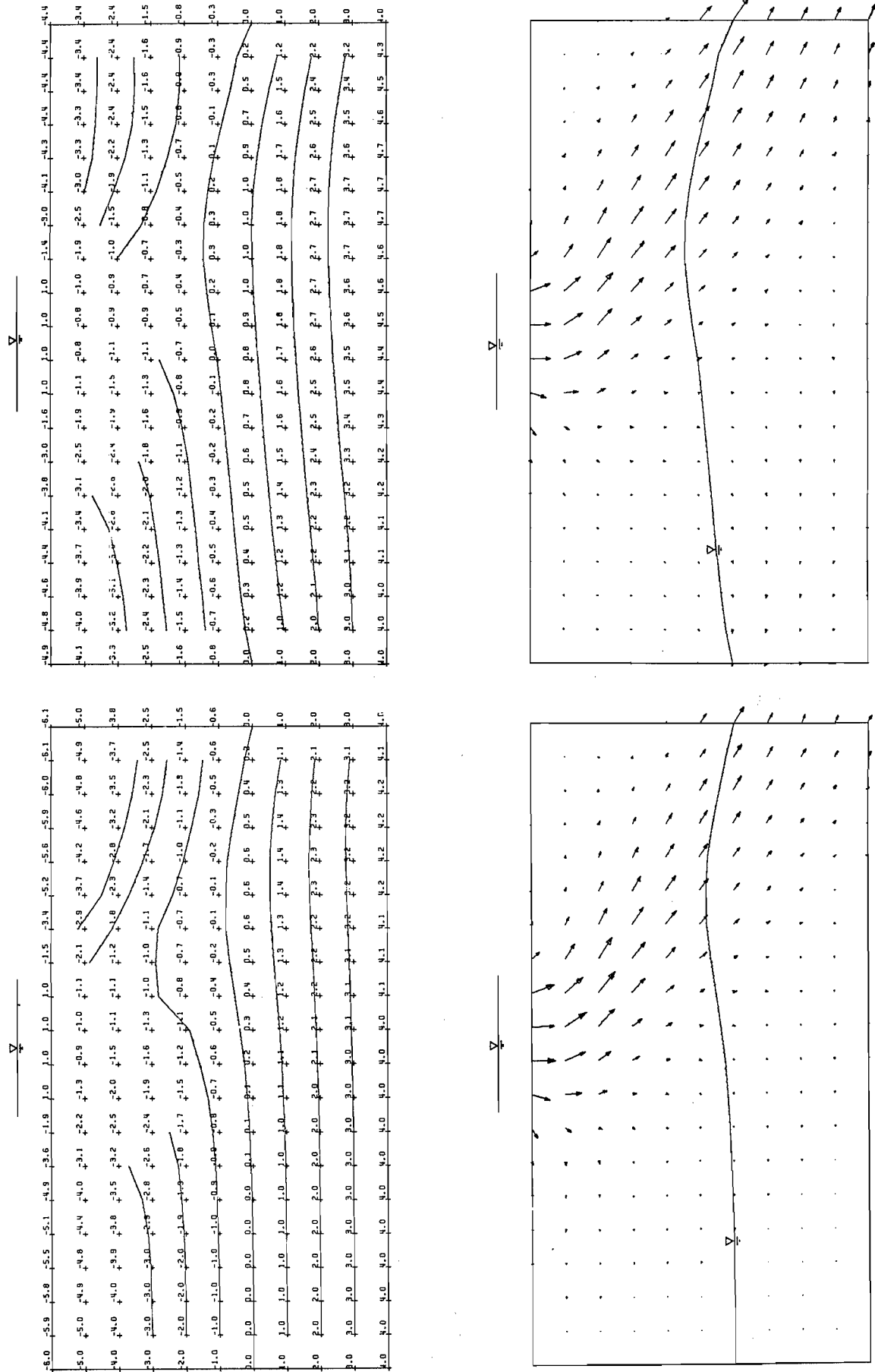
ing from the right boundary is substantially higher than that from the left boundary because of anisotropy.

Rulon and Freeze (1985) studied the steady state seepage of a layered hill slope under constant infiltration conditions. A sandbox model of the layered hill slope was constructed and elaborately monitored. The sandbox model was composed of medium sand, within which there was a horizontal layer of fine sand. The fine sand was to impede flow and create a seepage face on the slope. A constant infiltration was imposed on the top portion of the hill slope. The observed results were then calibrated using Neuman's finite element model called UNSAT I. The calibrated permeability values were 1.4×10^{-3} m/s for the medium sand and 5.5×10^{-5} m/s for the fine sand. The calibrated material permeabilities and an infiltration rate of 2.1×10^{-4} m/s produced a close comparison between the observed measurement and the results predicted by UNSAT I (Fig. 14).

The third example, 3, simulates the same layered hill slope problem using the developed model. Instead of solving only the steady state condition, the transient solution of the hill slope under infiltration was simulated. Figure 15 depicts the geometry and the boundary conditions of the sandbox model. The same permeability values and infiltration rate obtained by Rulon and Freeze (1985) were used in the transient simulation. An m_2^w value of 0.0005 m^2/kN as estimated from the moisture



(a) $t = 22.5$ min (b) $t = 66.5$ min
 FIG. 12. Nodal water pressure head and velocity vector plots at $t = 22.5$ and 66.5 min.



(a) $t = 174$ min

(b) $t = 1316$ min

Fig. 13. Nodal water pressure head and velocity vector plots at $t = 174$ and 1316 min.

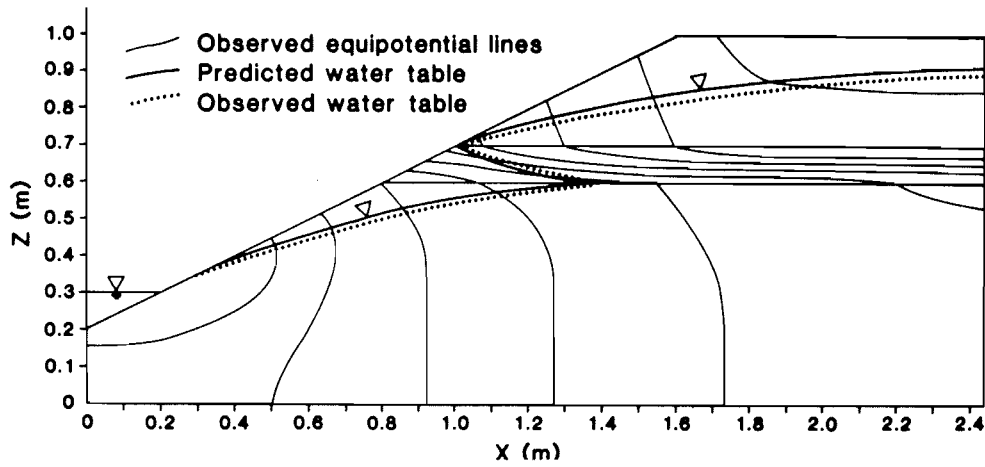


FIG. 14. Comparison of observed water table configuration in experimental sand tank with that predicted by Neuman's model, UNSAT I (after Rulon and Freeze 1985).

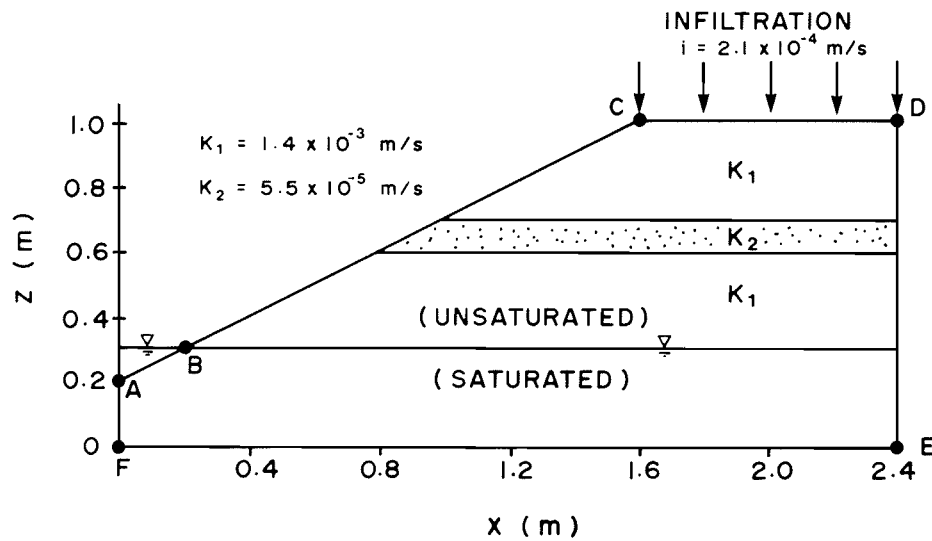


FIG. 15. Geometry and boundary conditions of example 3, seepage in layered hill slope.

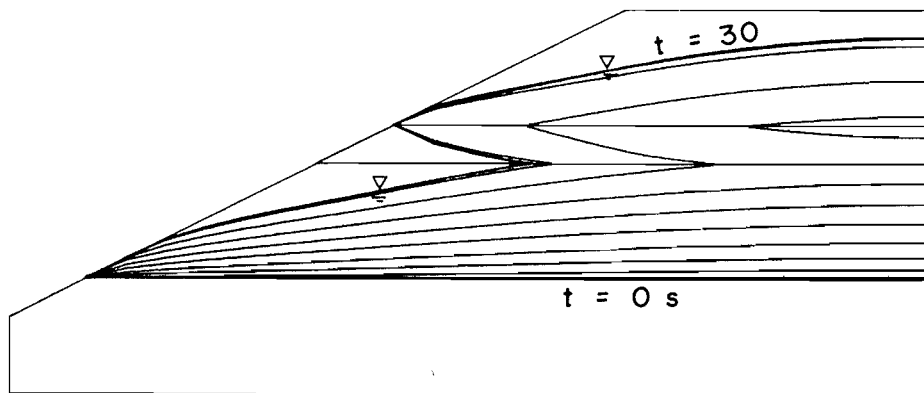
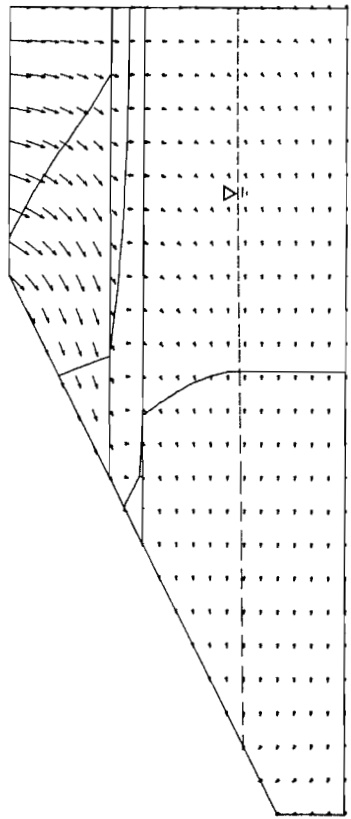


FIG. 16. Transient position of water table from $t = 0$ to $t = 30$ s.

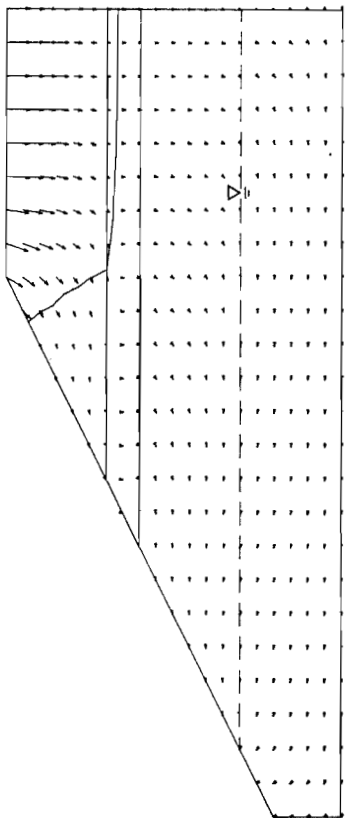
retention curve was used to represent the storage characteristic of the soils. An initial steady state condition was assumed with the water table located at 0.3 m. At time equal to zero, a constant infiltration rate was imposed on the top portion of the hill slope.

Figure 16 illustrates the development of the water table from its initial steady state condition to its final steady state condition. Figures 17 and 18 present the seepage velocity vector plots at various times after infiltration commenced.

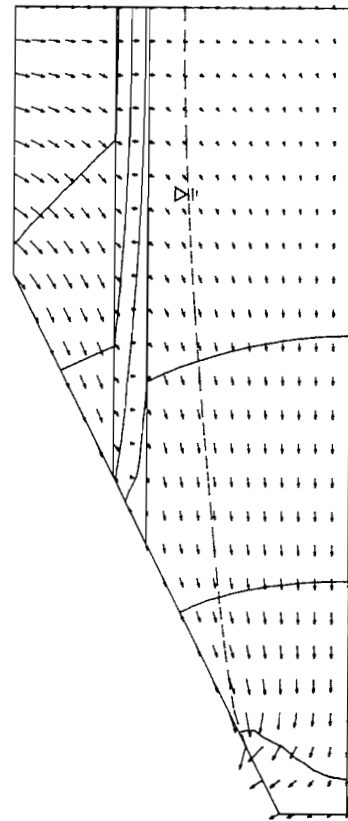
The results indicate that the presence of the impeding layer



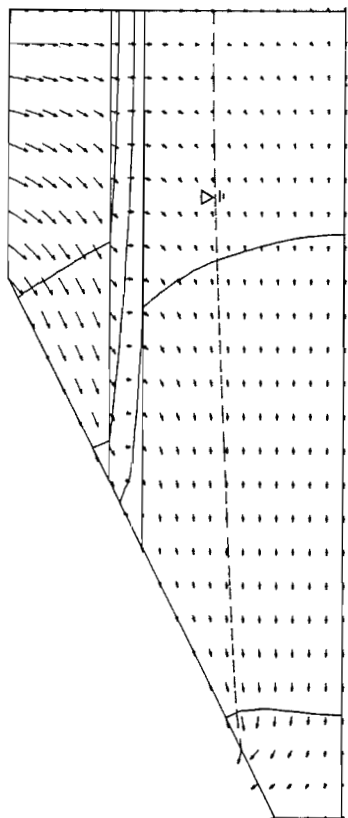
(a) $t = 1 \text{ s}$



(b) $t = 2 \text{ s}$

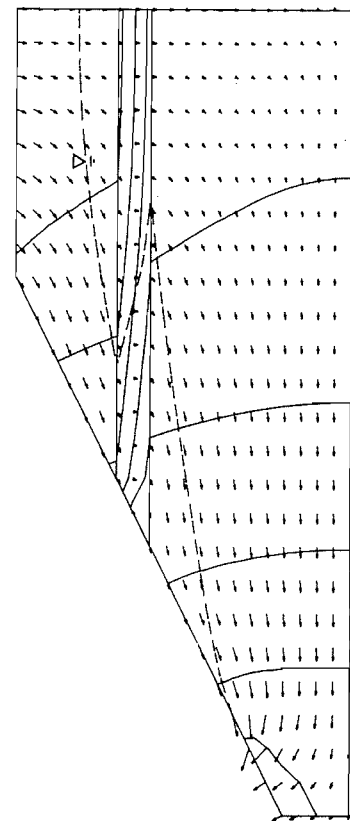


(c) $t = 5 \text{ s}$

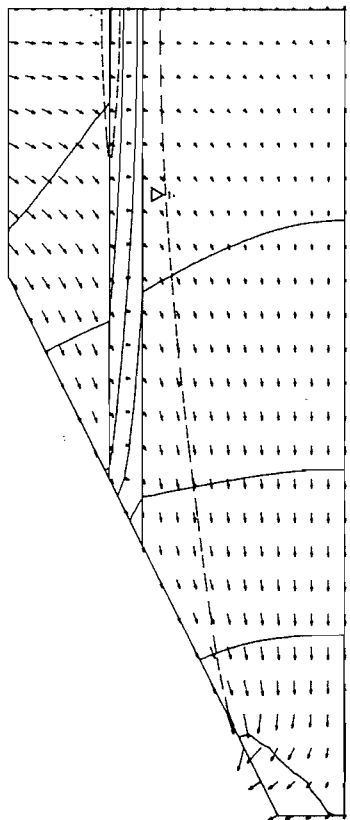


(d) $t = 8 \text{ s}$

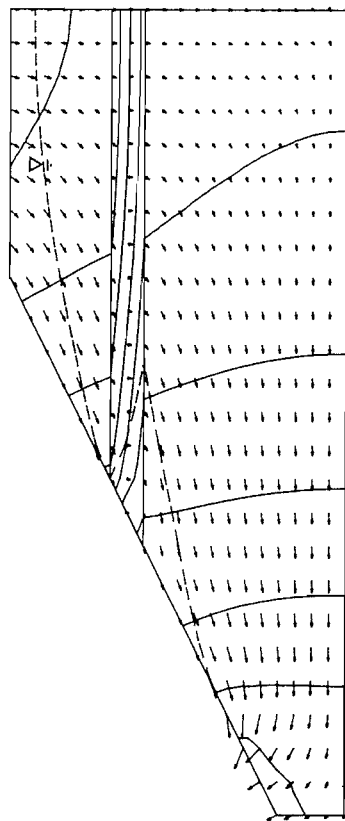
FIG. 17. Velocity vector plots at $t = 1, 2, 5,$ and 8 s .



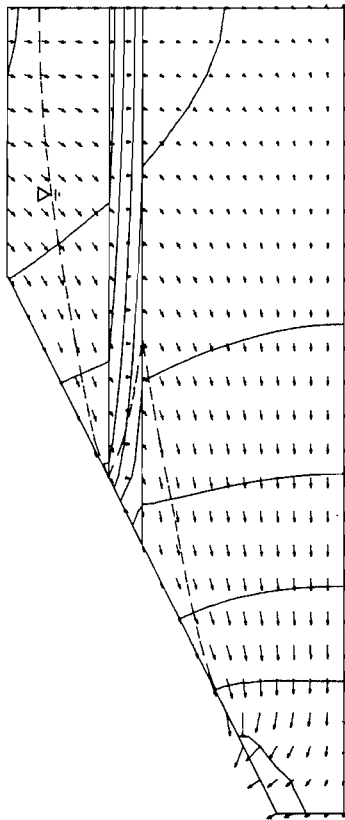
(a) $t = 10 \text{ s}$



(b) $t = 12 \text{ s}$



(c) $t = 16 \text{ s}$



(d) $t = 30 \text{ s}$

FIG. 18. Velocity vector plots at $t = 10, 12, 16,$ and 20 s .

creates a complex configuration to the position of the water table and the equipotential lines. At a time equal to 1 s, water infiltrates vertically toward the impeding layer, and the water table is essentially unaffected (Fig. 17a). The water table begins to rise at 2 s after infiltration commences (Fig. 17b). A perched water table on the impeding layer occurs at a time equal to 10 s (Fig. 18a). At a time equal to 12 s, part of the impeding layer is saturated and a wedge-shaped unsaturated zone is formed (Fig. 18b). After 16 s, two seepage faces develop, one near the toe of the hill slope, the other just above the impeding layer (Fig. 18c). Finally, at 30 s, a steady state condition is achieved (Fig. 18d).

The computed final steady state results (Fig. 18d) are compared with the steady state results (Fig. 14) presented by Rulon and Freeze (1985). A close agreement between the two sets of results can be observed. The water table position and the developed seepage faces in both figures are almost identical. In other words, the numerical result computed using TRASEE compared closely with the numerical result computed using the UNSAT I model and the experimental result obtained by Rulon and Freeze (1985).

The developed model TRASEE is fundamentally different than the model UNSAT I. UNSAT I seeks a solution in terms of pressure head. The governing partial differential equation is derived using a soil science approach. The storage characteristics of a material was expressed in terms of specific storage, S_s , and specific moisture capacity, C . TRASEE, however, seeks a solution in terms of total head, the governing partial differential equation is derived using a soil mechanics approach, and the storage characteristic of the material is expressed in terms of the water coefficient of volume change, m_v^w , as defined by Fredlund and Morgenstern (1976). Consequently, the transient solutions as predicted by the two models may be different; however, the steady state solutions should be the same.

Example 3 is also a class of seepage problem to which it is difficult to apply conventional saturated-only methods of analysis. The computed seepage velocity vectors indicate that water flows primarily in the unsaturated zone in the early stage of the infiltration process. Flow systems such as the above example can be complex depending on the position of the impeding layer and the permeability contrast between the soils. Features such as a perched water table, wedge-shaped unsaturated zones, and multiple seepage faces are difficult to handle without using a general saturated-unsaturated numerical model.

Conclusions and applications

The proposed finite element model offers a versatile tool for the analysis of a wide variety of seepage problems. Since water flow in both the saturated and unsaturated zones is considered, there is no assumption required with respect to the phreatic line in unconfined seepage problems. Results from the examples indicate that the phreatic line is not a flow line since there can be considerable water flow across the phreatic line. Furthermore, the quantity of water flow in the unsaturated zone may be substantial and failure to include the unsaturated zone may lead to unrealistic results.

Casagrande's flow-net solution and the traditional saturated-only flow models are shown to be a special case of the saturated-unsaturated flow model. The saturated-unsaturated model provides a more realistic and comprehensive representation of actual conditions. It can also be applied to a much wider range of engineering problems.

The computed results can be particularly valuable to practicing geotechnical engineers. The computed pore-water pressures throughout the flow region can be used to better understand the stress state in the soil. The stresses can then be applied in designs and analyses such as slope stability analyses. Saturated-unsaturated flow models can also be of value in the design of dams and storage lagoons. The computed flow gradients in a region allow the calculation of critical points where gradients may be excessive. The computed seepage flux through a section is also of value in the designs of engineering structures such as drains, cutoffs, and liners. The defined seepage velocities throughout the region permit the determination of critical flow paths and serve as input to contaminant transport modelling (Lam and Barbour 1985).

- BRAHMA, S. P., and HARR, M. E. 1962. Transient development of the free surface in a homogeneous earth dam. *Géotechnique*, **12**: 283–302.
- CASAGRANDE, A. 1937. Seepage through dams. *New England Water Works*. **51**(2): 131–172.
- CHILDS, E. C., and COLLIS-GEORGE, N. 1950. The permeability of porous materials. *Proceedings of the Royal Society of London*, **201**: 392–405.
- ELZEFATY, A., and CARTWRIGHT, K. 1981. Evaluating the saturated and unsaturated hydraulic conductivity of soils. *In Permeability and groundwater contaminant transport*. Edited by T. F. Zimmie, and C. D. Riggs. American Society for Testing and Materials, Special Technical Publication 146, pp. 168–181.
- FREDLUND, D. G. 1981. Seepage in unsaturated soils. Panel discussion: Groundwater and seepage problems. Tenth International Conference on Soil Mechanics and Foundation Engineering, Stockholm, Sweden.
- FREDLUND, D. G., and MORGENSTERN, N. R. 1976. Constitutive relations for volume change in unsaturated soils. *Canadian Geotechnical Journal*, **13**: 261–276.
- . 1977. Stress state variables for unsaturated soils. *ASCE Journal of the Geotechnical Engineering Division*, **103**(GT5): 447–466.
- FREEZE, R. A. 1971a. Three-dimensional transient saturated-unsaturated flow in a groundwater basin. *Water Resources Research*, **7**: 347–366.
- . 1971b. Influence of the unsaturated flow domain on seepage through earth dams. *Water Resources Research*, **7**(4): 929–940.
- FREEZE, R. A., and CHERRY, J. A. 1979. *Groundwater*. Prentice Hall, Englewood Cliffs, NJ.
- GREEN, R. E., and COREY, J. C. 1971. Calculation of hydraulic conductivity: A further evaluation of some predictive methods. *Soil Science Society of America Proceedings*, **35**: 3–8.
- HO, P. G. 1979. The prediction of hydraulic conductivity from soil moisture suction relationship. B.Sc. thesis, University of Saskatchewan, Saskatoon, Sask.
- LAM, L. 1983. Saturated-unsaturated transient finite element seepage model. M.Sc. thesis, University of Saskatchewan, Saskatoon, Sask.
- . 1984. Transient finite element seepage program, TRASEE. User's manual, CD-18, University of Saskatchewan, Saskatoon, Sask.
- LAM, L., and BARBOUR, S. L. 1985. Saturated-unsaturated mass transport modelling by finite element method. *Proceedings of 7th Symposium on Management of Uranium Mill Tailings. Low-Level Waste and Hazardous Waste*, Colorado State University, Fort Collins, CO, pp. 431–440.
- MARSHALL, T. J. 1958. A relation between permeability and size distribution of pores. *Journal of Soil Science*, **9**: 1–8.
- MCWHORTER, D. B., and NELSON, J. O. 1979. Unsaturated flow beneath tailings impoundments, *ASCE Journal of the Geotechnical Engineering Division*, **105**(GT11): 1317–1334.
- NEUMAN, S. P. 1973. Saturated-unsaturated seepage by finite ele-

- ments. ASCE Journal of the Hydraulics Division, **99**(HY12): 2233–2250.
- NEUMAN, S. P., and WITHERSPOON, P. A. 1971. Analysis of non-steady flow with a free surface using the finite element method. Water Resources Research, **7**: 611–623.
- PAPAGIANAKIS, A. T., and FREDLUND, D. G. 1984. A steady state model for flow in saturated–unsaturated soils. Canadian Geotechnical Journal, **21**: 419–430.
- RICHARDS, L. A. 1931. Capillary conduction of liquids through porous mediums. Physics (New York), **1**: 318–333.
- RULON, J. J., and FREEZE, R. A. 1985. Multiple seepage faces on layered slopes and their implications for slope-stability analysis. Canadian Geotechnical Journal, **22**: 347–356.
- TAYLOR, R. L., and BROWN, C. B. 1967. Darcy flow with a free surface. ASCE Journal of the Hydraulics Division, **93**(HY2): 25–33.
- TERZAGHI, K. 1943. Theoretical soil mechanics. John Wiley and Sons, New York, NY.